Supporting Information

Xiong et al. 10.1073/pnas.1712648115

SI Materials and Methods

Animals. Mice were housed and treated in accordance with the NIH *Guide for the Care and Use of Laboratory Animals* (1) and institutional animal care and use committees of Johns Hopkins University and the National Cancer Institute. Animals were housed in a 12-h dark and light cycle with free access to water and food. Colonies were established, and male and female animals were assigned to groups by computer-generated randomization. Sample size was justified by power analysis.

Generation of TH-tTA Transgenic Mice. We constructed a hTH-tTA vector in which the human TH promoter (11 kb) drives expression of tTA and a fluorescent reporter, zsGreen. Briefly, a tTA-IRES-zsGreen PCR fragment (amplified from a template, pTet-DualOFF; Clontech) was cloned into the hTH-hTorsinA construct in which hTorsinA was removed by double digestion with AgeI and HpaI (gift from Michelle E. Ehrlich, Icahn School of Medicine at Mount Sinai, New York) (2, 3). The transgenic constructs were linearized by the AflII/NotI enzymes and subsequently microinjected into the embryos of B6C3F2 mice. One- or two-cell embryos were transferred into B6D2F1 pseudopregnant female mice. Genomic DNA was prepared from tail snip [Proteinase K (Roche Diagnostics); direct PCR tail lysis (Viagen)], and pups were genotyped by PCR (DreamTaq Green Master Mix; Thermo Scientific) by using TH-tTA primers (forward, acc ctg tac tgg cac gtg aag; reverse, gca tag aat cgg tgg tag gtg; PCR product, 382 bp). Positive founders were selected and further subjected to semiquantitative PCR and normalized to GAPDH PCR (forward, AAA CCC ATC ACC ATC TTC CAG; reverse, AGG GGC CAT CCA CAG TCT TCT; PCR product, 300 bp) to screen for high copy-number founders. The three highest-copy founders were selected and backcrossed with C57/BL6 mice for more than 10 generations and to establish the transgenic lines.

TEM. TEM was performed on mouse brain slices at the microscope facility at The Johns Hopkins University School of Medicine. Mice were perfused with PBS solution containing 1% sodium nitrite (pH 7.4), followed by fixation with fixative consisting of 3% (vol/vol) paraformaldehyde, 1.5% (vol/vol) glutaraldehyde, 100 mM cacodylate, and 2.5% (vol/vol) sucrose (pH 7.4), and postfixed for 1 h. Brain sections were processed and imaged as described previously (4). Images were collected on a Philips EM 410 transmission electron microscope installed with a Soft Imaging System Megaview III digital camera.

Immunohistochemistry. Mice were perfused with ice-cold PBS solution followed by ice-cold 4% PFA (Sigma-Aldrich)/PBS solution (pH 7.4). Brains were removed and postfixed overnight at 4 °C in the same fixative and then transferred to 30% sucrose/PBS solution at 4 °C for cryoprotection. Once saturated in sucrose, brains were frozen on dry ice and serial coronal sections (40 μm) were cut by a microtome. To allow antigen retrieval, brain sections were incubated with 10 mM sodium citrate (pH 6.0) with 0.05% Tween-20 for 30 min at 37 °C. After washing with PBS solution three times, brain sections were blocked for 1 h with PBS solution containing 10% goat serum (Sigma-Aldrich) and 0.3% Triton X-100 (blocking buffer). After washing with PBS solution, sections were incubated with indicated primary antibodies diluted in blocking buffer at 4 °C overnight. After washing with PBS solution, brain sections were incubated with goat anti-mouse IgG conjugated to Alexa Fluor-594 or -488 or goat anti-rabbit IgG conjugated to Alexa Fluor-488 or -594 (Thermo Fisher) at room temperature for 2 h. Coverslips were mounted onto slides using Vectashield mounting medium with DAPI (Vector Laboratories). Imaging was conducted on a Zeiss confocal 700 or 880 microscope (Carl Zeiss).

Stereological assessment of TH- and Nissl-Positive Cells. Brain sections were prepared as described in the previous section. Every four sections were collected for subsequent procedures. Free-floating sections were blocked for 1 h with PBS solution containing 10% goat serum (Sigma-Aldrich) and 0.3% Triton X-100 (blocking buffer). After washing with PBS solution, the sections were incubated with TH antibodies diluted in blocking buffer at 4 °C overnight. After washing with PBS solution, brain sections were incubated with biotin-conjugated antibody to rabbit, ABC reagents (Vector Laboratories), and Sigmafast 3,3-diaminobenzidine tablets (Sigma-Aldrich). Sections were counterstained with Nissl (0.09% thionin) after TH staining as previously described (5–7). Sections were dehydrated in 100% ethanol and cleared in xylene (Fisher Scientific) followed by mounting with DPX (Sigma-Aldrich). TH-positive and Nissl-positive DA neurons from the SNpc region were imaged and counted through an optical fractionator. This unbiased stereological counting was carried out by a computer-assisted image-analysis system consisting of an Axiophot photomicroscope (Carl Zeiss Vision) equipped with a computer-controlled motorized stage (Ludl Electronics), an HV C20 video camera (Hitachi), and Stereo Investigator software (MicroBrightField).

Monoamine Analysis by HPLC-ECD. Monoamine concentrations were measured by HPLC-ECD as previously described (6). Briefly, mice were killed by decapitation, and the STR or CER was quickly removed. Tissues were sonicated in ice-cold 0.01 mM perchloric acid containing 0.01% EDTA and 60 ng 3,4-dihydroxybenzylamine as an internal standard. The lysate was centrifuged at 15,000 × *g* for 30 min at 4 °C. The supernatant was cleared by a 0.2-μm filter and analyzed in the HPLC column (4.6 mm × 150 mm C-18 reverse-phase column, 3 μM; Atlantis T3) by a dual-channel Coulochem III electrochemical detector (model 5300; ESA). Data were normalized to protein concentrations and expressed in nanograms per milligram protein as previously described (6).

Antibodies. Primary antibodies used in this study are as follows: rabbit anti-LRRK2 (ab133474, MJFF C41-2; Epitomics/Abcam) for immunohistochemistry, mouse anti-LRRK2 antibody (N136/8; NeuroMab RRID:AB_2234791), rabbit anti-LRRK2 antibody (1304; D18E12; Cell Signaling Technology) recognizing mouse and human LRRK2, rabbit anti-LRRK2 phospho-Ser1292 antibody (ab203181; MJFR-19–7-8; Abcam), rabbit anti-TH (NB300-109, RRID:AB_350437; Novus Biologicals), rabbit anti-GFAP (Z0334, RRID:AB_10013382; Dako), mouse anti–α-synuclein antibody (610787; RRID:AB_398108; BD Transduction Laboratories), rabbit anti–α-synuclein antibody (2642; RRID:AB_2192679; Cell Signaling Technology), mouse anti-pS129 α-synuclein (015-25191, RRID:AB_2537218; Wako), rabbit anti-zsGreen (632474, RRID:AB_2491179; Clontech), and mouse anti-CD68 (NB100-683, RRID:AB_2074852; Novus Biological). Secondary antibodies used in this study are goat anti-mouse IgG conjugated to Alexa Fluor-594 or -488 (Thermo Fisher) or goat anti-rabbit IgG conjugated to Alexa Fluor-488 or -594 (Thermo Fisher) for immunohistochemistry and anti–Actin-peroxidase (A3854; RRID:AB_262011; Sigma-Aldrich) for Western blot loading controls.

Western Blotting. Brain tissue from the indicated genotype was homogenized in lysis buffer [1 × PBS solution, 1% Triton X-100, 1 × Complete protease inhibitor (4693116001; Sigma), 1 × PhosSTOP phosphatase inhibitor (4906845001; Sigma)]. Protein concentrations of tissue homogenates were measured by BCA protein assay kit (Pierce). Protein (100 μg) was resolved by SDS/PAGE, transferred to PVDF membranes, and probed with indicated antibodies. Densitometric analysis was conducted. Total protein levels were normalized to actin.

Mouse Behavioral Tests.

Open-field test and d-amphetamine administration. Spontaneous locomotor and exploratory activities were assessed as described in our recent paper (5). Briefly, a mouse was placed in the center of the open-field arena and allowed to explore the area for 25 min followed by saline solution administration. The mouse was allowed to explore for another 25 min, followed by d-amphetamine administration (7 mg/kg s.c.; A-5880; lot no. 34H0145; Sigma-Aldrich). The mouse was allowed to explore for another 25 min. The activities of a mouse were recorded every 1 min by Photobeam Activity System software installed on a computer connected to the open-field equipment. Before and after each testing, the clear acrylic enclosure of the surface of the arena was cleaned with 70% ethanol. The total number of beam breaks during the total 50-min period was analyzed to determine gross locomotor activity of the mouse.

Rotarod test. The rotarod test was performed as described in our recent paper (5). Briefly, motor coordination of mice was measured as the retention time on an accelerating rotarod of the Rotamex V instrument equipped with photo beams and a sensor to automatically detect mice that fell from the rotarod (Columbus Instruments). Before the actual test, the mice were trained on the rotarod at 4.0–40 rpm for 5 min and allowed to rest for at least 30 min. The training occurred over three consecutive days and consists of three test trials. On the day of the test, four mice were placed on separate rods, and the durations on the accelerating rods were recorded automatically by the software installed on a computer connected to the instrument. Rotamex instrument settings were as follows: start speed, 4.0 rpm; maximum speed, 40 rpm; acceleration interval, 30 s; and acceleration step, 4 rpm. The settings remained constant throughout all trials. The tests were blinded and evaluated in three sessions, and the average retention time and end speed were recorded for each mouse. The motor coordination of the mouse was determined by the retention time.

Pole test and L-Dopa administration. The pole test was performed as described previously (5). The pole consists of a 9-mm-diameter, 2.5-foot metal rod wrapped with bandage gauze. Briefly, the mice were placed 3 inches from the top of the pole facing head-up. Total time taken to turn and reach the base of the pole was recorded. Before the actual test, the mice were trained for three consecutive days, and each training session consisted of three test trials. On the day of the test, mice were evaluated in three sessions with 1-h intervals in between. The tests were blinded, and results were expressed in total time in seconds (5, 6). Mice with indicated genotypes were injected i.p. with saline solution control or 20 mg/kg body weight methyl–L-Dopa hydrochloride (Sigma) in 0.9% NaCl with 6.5 mg/kg benserazide (Sigma). Pole tests were performed 40 min after the injections.

Gait analysis. The gait analysis was performed by footprint analysis. Briefly, front and hind paws of the test animals were dipped in yellow and blue nontoxic water-soluble paint, respectively, and the mice were allowed to walk on a replaceable strip of white paper. Before the actual test, the mice were trained for three consecutive days, and each training session consisted of three test trials. The stride length and stride width were measured.

1. National Research Council (2011) *Guide for the Care and Use of Laboratory Animals* (National Academies Press, Washington, DC), 8th Ed.
2. Kessler MA, Yang M, Gollomp KL, Jin H, Iacovitti L (2003) The human tyrosine hydroxylase gene promoter. *Brain Res Mol Brain Res* 112:8–23.
3. Page ME, et al. (2010) Cell-autonomous alteration of dopaminergic transmission by wild type and mutant (DeltaE) TorsinA in transgenic mice. *Neurobiol Dis* 39:318–326.
4. McCaffery JM, Farquhar MG (1995) Localization of GTPases by indirect immunofluorescence and immunoelectron microscopy. *Methods Enzymol* 257:259–279.
5. Xiong Y, et al. (2017) Overexpression of Parkinson's disease-associated mutation LRRK2 G2019S in mouse forebrain induces behavioral deficits and α-Synuclein pathology. *eNeuro* 4:ENEURO.0004-17.2017.
6. Karuppagounder SS, et al. (2016) LRRK2 G2019S transgenic mice display increased susceptibility to 1-methyl-4-phenyl-1,2,3,6-tetrahydropyridine (MPTP)-mediated neurotoxicity. *J Chem Neuroanat* 76:90–97.
7. Lee Y, et al. (2013) Parthanatos mediates AIMP2-activated age-dependent dopaminergic neuronal loss. *Nat Neurosci* 16:1392–1400.

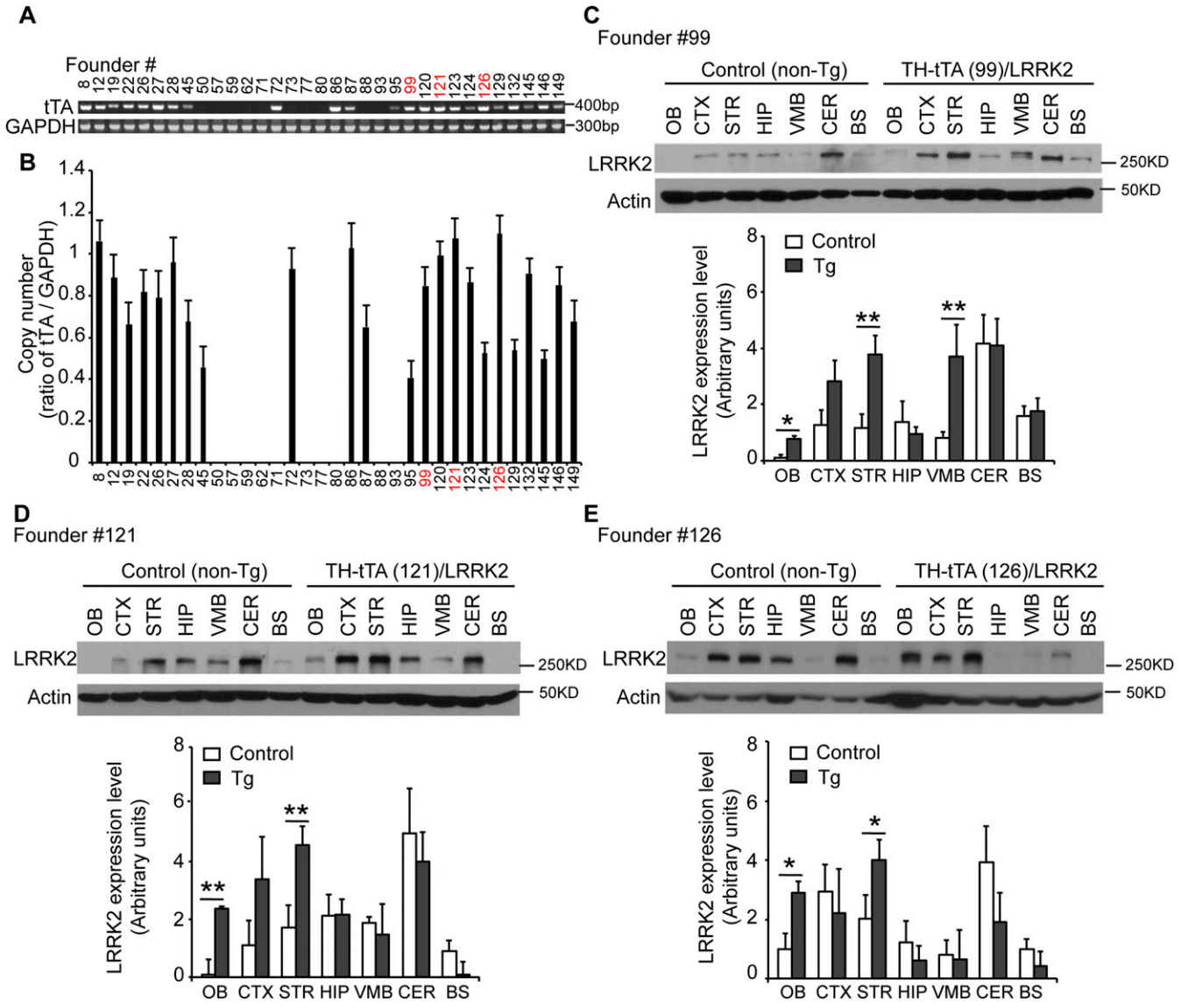

Fig. S1. TH-tTA transgenic founder mouse screening. (*A*) Representative genotyping PCR for hTH-tTA using tail genomic DNA. GAPDH PCR was used as an internal control. (*B*) Relative transgene copy number determined by semiquantitative PCR performed on genomic DNA expressed in arbitrary units as the ratio of the hTH-tTA transgene to GAPDH for each founder mouse. (*C–E*) Representative Western blots of LRRK2 distribution in brain subregions from double transgenic mice with hTH-tTA founder mouse no. 99 (*C*), no. 121 (*D*), and no. 126 (*E*) crossed with TetP-LRRK2-GS no. 569 mouse (BS, brainstem), and quantification data of LRRK2 distribution in mouse brains normalized to β-actin ($n = 3$). Data are the mean ± SEM. A statistically significant difference between groups was determined by two-way ANOVA [no. 99, $F(6,28) = 6.362$, $P = 0.0003$; no. 121, $F(6,28) = 4.147$, $P = 0.0042$; no. 126: $F(6,28) = 3.193$, $P = 0.0163$] followed by a Tukey's post hoc test (*$P < 0.05$ and **$P < 0.01$).

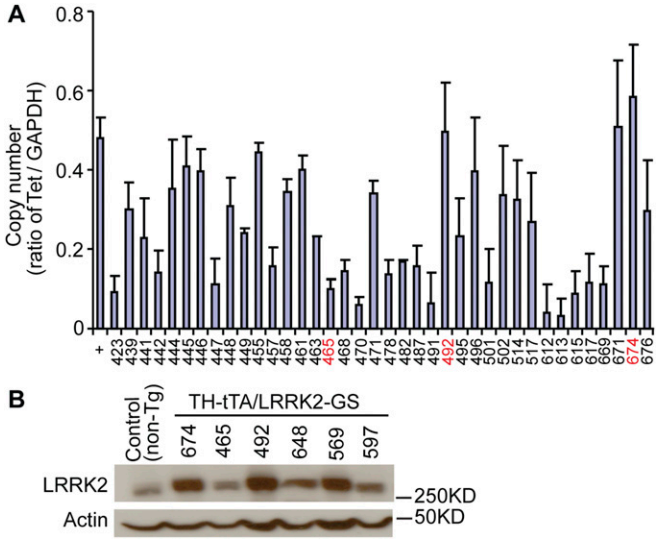

Fig. S2. Screening of additional Tet-inducible conditional LRRK2 transgenic mice. (*A*) Relative transgene copy number determined by semiquantitative PCR performed on genomic DNA expressed in arbitrary units as the ratio of the TetP-LRRK2-G2019S (GS) transgene to GAPDH for each founder mouse. (*B*) Western blot analysis of LRRK2 expression from TH-tTA/LRRK2 GS transgenic mouse brain. Each number represents a single LRRK2 transgenic founder line.

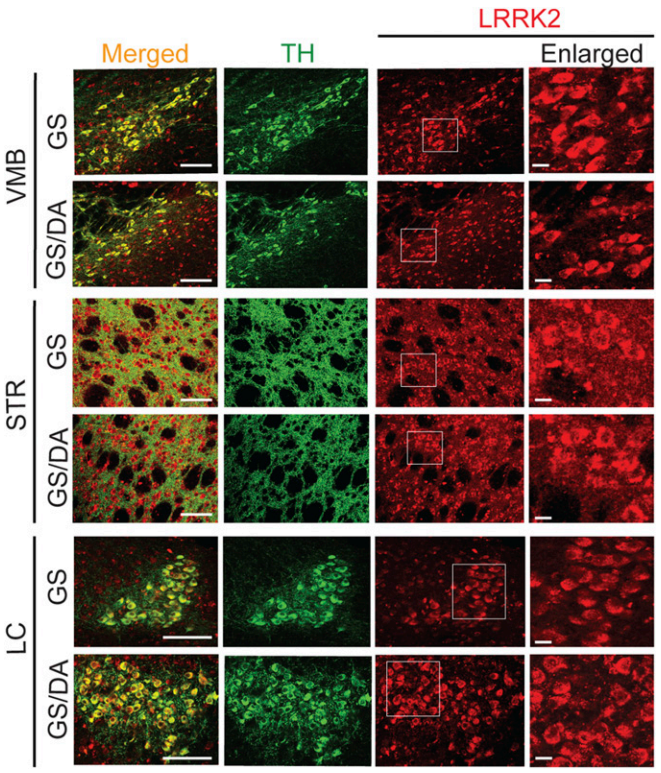

Fig. S3. LRRK2 expression level in LRRK2 transgenic mouse brain. Immunohistochemistry images of LRRK2 (red) and TH (green) at VMB, STR, and LC subregions from coronal sections of LRRK2 GS and GS/DA transgenic mice. (Scale bars: low-magnification images, 100 μm; high-magnification images, 20 μm.)

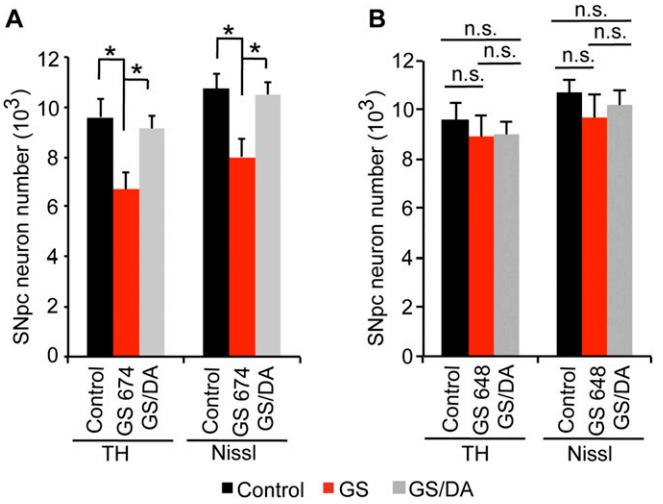

Fig. S4. Characterization of DA neurodegeneration at SNpc in conditional LRRK2 GS 674 and 648 line. (*A*) Stereological assessment of TH- and Nissl-positive neurons in the SNpc in LRRK2 GS 674 line ($n = 5$). A statistically significant difference between groups as determined by one-way ANOVA [TH, $F(2,12) = 6.219$, $P = 0.014$; Nissl, $F(2,12) = 5.498$, $P = 0.0202$] followed by Tukey's post hoc test. (*B*) Stereological assessment of TH- and Nissl-positive neurons in the SNpc in LRRK2 GS 648 line ($n = 8$). There was no statistically significant difference between groups as determined by one-way ANOVA [TH, $F(2,21) = 0.2852$, $P = 0.7547$; Nissl, $F(2,21) = 0.5282$, $P = 0.5973$] followed by Tukey's post hoc test. Data are the mean ± SEM (*$P < 0.05$; n.s., not significant).

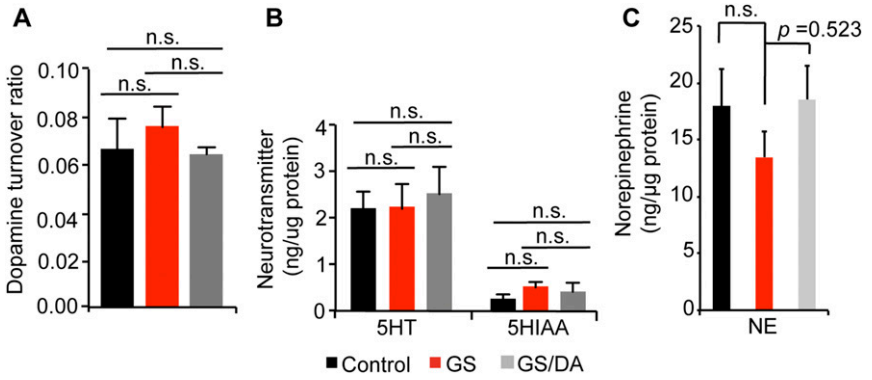

Fig. S5. Striatal DA metabolites levels were analyzed by HPLC. (*A*) DA turnover in the STR was analyzed by HPLC in controls and LRRK2 GS and GS/DA transgenic mice at 24 mo of age. There was no statistically significant difference between groups as determined by one-way ANOVA [$F(2,6) = 1.514$, $P = 0.2935$] followed by a Tukey's post hoc test. (*B*) 5HT and 5HIAA levels were analyzed by HPLC in controls and LRRK2 GS and GS/DA transgenic mice at 24 mo of age. There was no statistically significant difference between groups as determined by one-way ANOVA [5HT, $F(2,6) = 0.3794$, $P = 0.6996$; 5HIAA, $F(2,6) = 2.588$, $P = 0.1547$] followed by Tukey's post hoc test. (*C*) NE levels in the CER were analyzed by HPLC in controls and LRRK2 GS and GS/DA transgenic mice at 24 mo old of age. There was no statistically significant difference between groups as determined by one-way ANOVA [$F(2,12) = 0.978$; $P = 0.4041$] followed by Tukey's post hoc test. Data are presented as the mean ± SEM (n.s., not significant). *P* values for post hoc tests for each comparison are reported in Table S1. n.s., not significant.

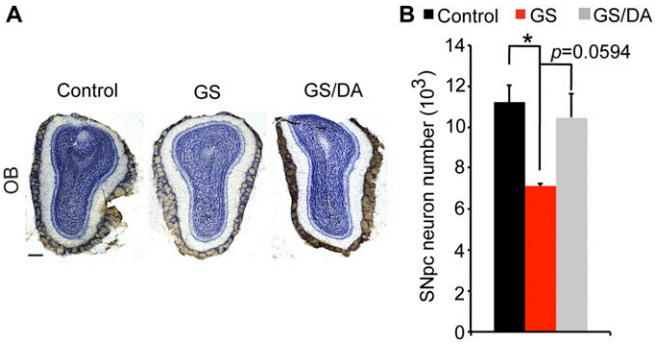

Fig. S6. Characterization of DA neurodegeneration in OB in conditional LRRK2 transgenic mice. (*A*) Representative TH immunohistochemistry of the OB coronal sections of 24-mo-old LRRK2 GS and GSDA transgenic and age-matched littermate controls. (Scale bar: 100 μm.) (*B*) Stereological assessment of TH-positive neurons in the OB ($n = 3$). A statistically significant difference between groups as determined by one-way ANOVA [$F(2,6) = 7.261$; $P = 0.025$] followed by a Tukey's post hoc test. Data are the mean ± SEM (*$P < 0.05$; n.s., nonsignificant).

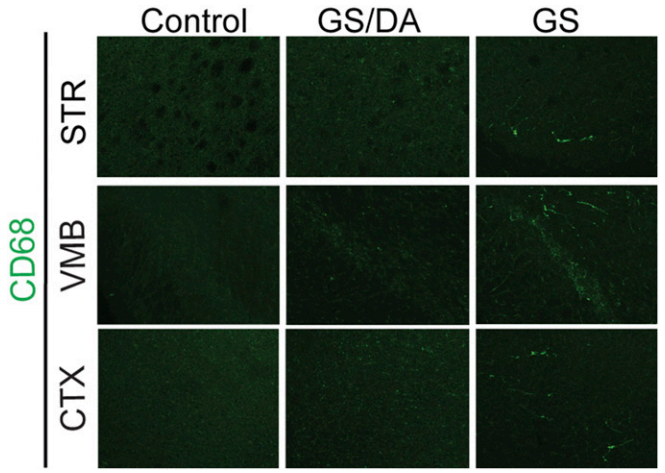

Fig. S7. Examination of microglia activation by CD68 immunostaining. Representative CD68 immunostaining (green) of the STR, VMB, and CTX coronal sections of 24-mo-old LRRK2 GS and GSDA transgenic and age-matched littermate controls. (Magnification: 20×.)

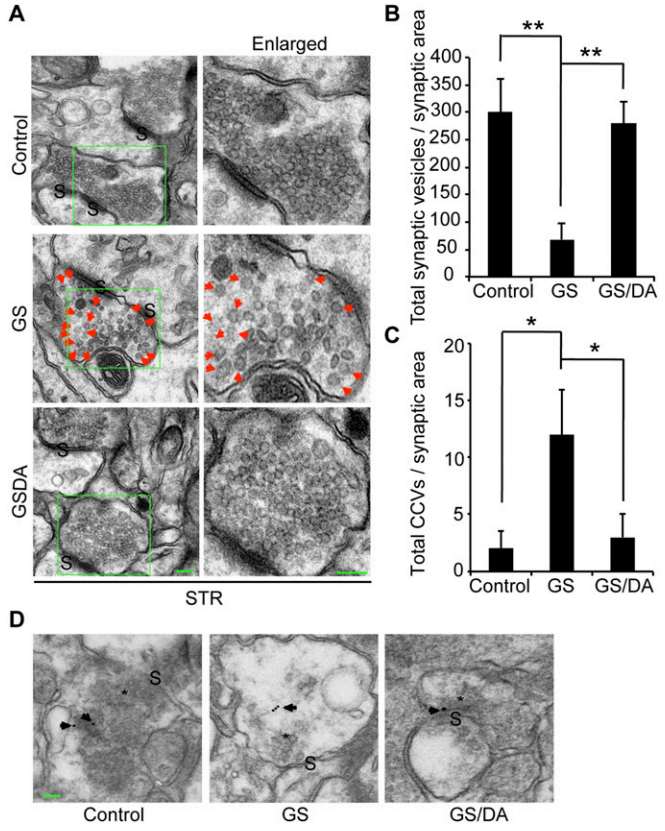

Fig. S8. Reduced SVs and accumulation of CCVs at DA terminals. (*A*) TEM ultrastructure of nerve terminals from STR of 24-mo-old LRRK2 GS and GS/DA transgenic and age-matched littermate controls. CCVs are indicated by red arrowheads (S, synapse). (Scale bars: 100 nm.) (*B*) Quantification of the number of SVs per synaptic area ($n = 30$). Significance was determined by one-way ANOVA [$F(2,87) = 8.129$; $P = 0.0006$] followed by Tukey's post hoc test. (*C*) Quantification of the number of CCVs per synaptic area ($n = 30$). Significance was determined by one-way ANOVA [$F(2,87) = 4.09$; $P = 0.0201$] followed by Tukey's post hoc test. Data are the mean ± SEM (*$P < 0.05$, **$P < 0.01$ and ***$P < 0.001$). (*D*) Immunogold VMAT2 staining of DA nerve terminals. TEM ultrastructure of nerve terminals from STR of 24-mo-old LRRK2 GS and GS/DA transgenic and age-matched littermate controls. Immunogold staining is indicated by black arrows (S, synapse). Synaptic vesicle clusters are indicated by stars (*). (Scale bar: 100 nm.)

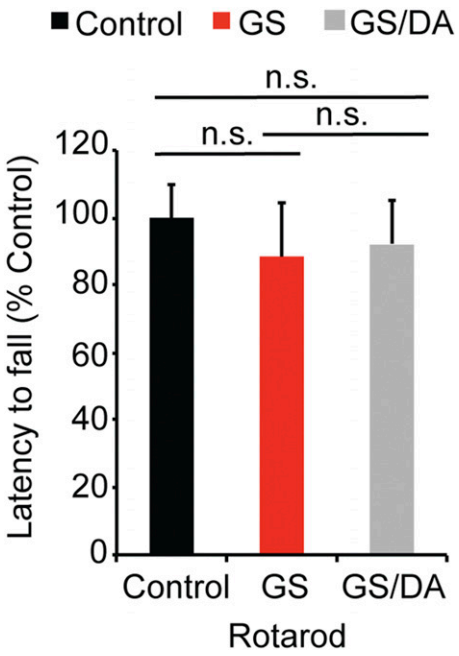

Fig. S9. Rotarod test of conditional LRRK2 transgenic mice. Assessment of latency to fall in an accelerated rotarod test (n = 8). There was no statistically significant difference between groups as determined by one-way ANOVA [$F(2,21) = 0.1958$; $P = 0.8237$] followed by a Tukey's post hoc test. Data are the mean ± SEM (n.s., not significant).

Other Supporting Information Files

Table S1 (DOCX)